Modied mean-field theory of one-dimensional spin models with anisotropy and long-range dipolar interactions

Modified mean-field theory of one-dimensional spin models with anisotropy and long-range dipolar interactions

Philip J. Camp*
School of Chemistry, University of Edinburgh, David Brewster Road, Edinburgh EH9 3FJ, Scotland and Department of Theoretical and Mathematical Physics, Institute of Natural Sciences and Mathematics, Ural Federal University, 51 Lenin Avenue, Ekaterinburg 620000, Russia

Alexey O. Ivanov
Department of Theoretical and Mathematical Physics, Institute of Natural Sciences and Mathematics, Ural Federal University, 51 Lenin Avenue, Ekaterinburg 620000, Russia and M. N. Mikheev Institute of Metal Physics UB RAS, 18 Sofia Kovalevskaya Street, Ekaterinburg 620109, Russia
(Dated: March 31, 2020)

The effects of interactions and anisotropy on the magnetic properties of linear chains of superparamagnetic nanoparticles are studied theoretically by mapping the problem onto spin models. With zero anisotropy, the magnetic dipole moments are free to rotate, and the system resembles a classical ferromagnetic Heisenberg model with long-range dipolar interactions. With strong anisotropy, they are constrained to align with the chain, and the system resembles a classical ferromagnetic Ising model with long-range interactions. Using a modified mean-field theory, expressions for the magnetization curve and initial magnetic susceptibility are derived from the response of a single particle subject to an effective field arising from the applied field and the interactions with the other particles. Various approximations for the effective field are tested against results from Monte Carlo simulations. It is shown that for physically relevant interaction strengths, reliable theoretical predictions for both the zero-anisotropy and strong-anisotropy cases can be derived in simple and closed form.

Keywords: Heisenberg model; Ising model; dipolar interactions; magnetization; magnetic susceptibility; modified mean-field theory; Monte Carlo simulations.

I. INTRODUCTION

A superparamagnetic nanoparticle possesses a net magnetic dipole moment $\boldsymbol{\mu}$ which is aligned preferentially along an easy axis defined by the crystal structure of the constituent material. The dipole moment can reorient through the Néel mechanism at a rate that depends on the energy barrier separating two degenerate orientations, which is characterized by the anisotropy constant K of the magnetic material. The Néel relaxation time is proportional to $\exp(\sigma)$, where $\sigma = Kv/k_{\mathrm{B}}T$, v is the volume of the magnetic core of the particle, k_{B} is Boltzmann's constant, and T is the temperature [1]. In a fluid colloidal suspension, the nanoparticles (and their easy axes) undergo Brownian rotation, and so the dipole moments can reorient by a combination of the Néel and Brownian mechanisms [1]. If the nanoparticles are immobilized in a solid matrix, then the Brownian mechanism is blocked, and the orientations of the easy axes are fixed. It is important to understand how the anisotropy and the orientational distribution of easy axes affect the magnetization curve and initial magnetic susceptibility of immobilized superparamagnetic nanoparticles, in order that new materials can be developed and exploited for technological applications [2, 3]. Recently, this problem was studied using a combination of theory and computer simulation [4]. The theory was based on the so-called modified mean-field (MMF) approach [5, 6], where the problem of interacting magnetic particles is reduced to a one-particle calculation by defining an effective magnetic field due to the applied field and the interactions with the other particles. To calculate this effective field requires a description of the orientational correlations between particles. In the first-order MMF theory, correlations are ignored. It was found that the MMF theory works well in the case of zero anisotropy ($\sigma = 0$) or when the easy axes are oriented randomly in space, as compared to numerical results from Monte Carlo (MC) simulations. The reason for this is that the effective interactions between dipoles are short ranged; although the dipolar interaction is anisotropic and decays with distance r like $1/r^3$, the longest-range part of the orientationally averaged, isotropic interaction decays like $-1/r^6$ [7]. Hence, the orientational correlations are weak, and a mean-field approach is adequate to compute the magnetic properties. The MMF approach is not very accurate in the case of strong anisotropy (large σ) and parallel alignment of the easy axes with the field direction. In this case, the interactions between dipoles remain anisotropic and long-ranged, the orientational correlations are substantial, and the impact on the magnetic properties is significant. To improve the accuracy of the MMF theory, a better rep-

* Corresponding author: philip.camp@ed.ac.uk

resentation of the orientational correlations is required.

In general, describing the orientational correlations between strongly interacting dipolar particles is difficult, but there is at least one special case where the problem can be simplified considerably. In the classical one-dimensional n-vector models [8], each spin $\boldsymbol{S}$ has n components, and the exchange energy is proportional to $-J\boldsymbol{S}_i \cdot \boldsymbol{S}_j$. The models with nearest-neighbor ferromagnetic interactions have been studied extensively, and the properties are known exactly: the Heisenberg model corresponds to $n = 3$ [9, 10]; and the Ising model corresponds to $n = 1$ [11]. With interactions that decay with distance like r^{-a}, the Heisenberg model only exhibits ferromagnetism if $1 < a < 2$ [12–14], and the Ising model exhibits ferromagnetism if $1 < \alpha \leq 2$ [15–19].

The ferromagnetic Ising model resembles a linear chain of immobilized superparamagnetic nanoparticles, with the easy axes aligned with the chain, an anisotropy constant $\sigma \to \infty$, and the magnetic field applied in the chain direction. The long-range dipolar interactions can be thought of as a perturbation to the nearest-neighbor interactions in the Ising model. Hence, in this special case, the effective field felt by one superparamagnetic nanoparticle in the chain could be estimated by using the properties of the one-dimensional Ising model. Something similar could be done for the $\sigma = 0$ case, but the necessary expressions for the one-dimensional Heisenberg model are much more complicated [10, 20].

This aim of this study is to compute the magnetic properties of a linear chain of interacting superparamagnetic nanoparticles by mapping the problem onto one-dimensional spin models. Simple formulas will be obtained describing the dependence of the magnetization curve and initial susceptibility on the strength of the interactions. The theoretical predictions will then be tested against numerical results from MC simulations. The rest of this article is organized as follows. Section II summarizes various MMF and mean-field (MF) approaches to the properties of systems with zero anisotropy ($\sigma = 0$, Heisenberg-like spins) and with infinite anisotropy ($\sigma = \infty$, Ising-like spins). Section III describes the MC simulations. The results are presented in Section IV, and Section V concludes the article.

II. THEORY

A. Model

N spins are equally spaced in a chain aligned with the z axis. The Hamiltonian $\mathcal{H}$ is given by

$$\beta\mathcal{H} = \sum_{i=1}^{N}\sum_{j>i}^{N} \beta U(\boldsymbol{S}_i, \boldsymbol{S}_j, r) + \sum_{i=1}^{N} \beta\Phi(\boldsymbol{S}_i) \tag{1}$$

where $\beta = 1/k_{\mathrm{B}}T$, U is the pair interaction energy, and Φ contains the interaction energy between a spin and the applied field, and in the case of anisotropy, a term constraining the spin to align with a particular axis. The function U depends on the separation between the spins, $r = |i - j|$, and can include a cut-off at separation R. $R = 1$ corresponds to nearest-neighbor interactions, while $R = \infty$ means long-range interactions. A three-component spin is defined by a polar angle θ and an azimuthal angle ϕ: $\boldsymbol{S}_i = (S_{ix}, S_{iy}, S_{iz}) = (\sin\theta_i \cos\phi_i, \sin\theta_i \sin\phi_i, \cos\theta_i)$. The dipolar interaction energy between spins is

$$\begin{aligned}\beta U(\boldsymbol{S}_i, \boldsymbol{S}_j, r) &= \frac{J}{2r^3}\left(\boldsymbol{S}_i \cdot \boldsymbol{S}_j - 3S_{iz}S_{jz}\right) \\ &= \frac{J}{2r^3}\left[\sin\theta_i \sin\theta_j \cos(\phi_i - \phi_j) - 2\cos\theta_i \cos\theta_j\right]\end{aligned} \tag{2}$$

if $r = |i - j| \leq R$, and it is zero otherwise. The coupling constant J is defined such that the minimum interaction energy between nearest neighbors is $-J$ (when $\cos\theta_i = \cos\theta_j = 1$). The single-spin energy is

$$\beta\Phi(\boldsymbol{S}_i) = -\alpha S_{iz} - \sigma S_{iz}^2 \tag{3}$$

where α is proportional to a magnetic field in the z direction, and σ constrains the spins to lie along the easy axis, which is taken to be the z axis. The fractional magnetization is

$$m = \int_{-1}^{1} \cos\theta \rho(\cos\theta) \mathrm{d}\cos\theta \tag{4}$$

where $\rho(\cos\theta)$ is the one-spin density, $\int_{-1}^{1} \rho(\cos\theta)\mathrm{d}\cos\theta = 1$, $m = 0$ means no alignment, and $m = \pm 1$ means complete alignment.

B. Mapping the model onto immobilized magnetic colloids

To make a connection with colloidal properties [1], each spin corresponds to a magnetic dipole moment $\boldsymbol{\mu} = \mu\boldsymbol{S}$, and the spacing between spins is a. For spherical superparamagnetic particles with diameter d, the dipolar coupling constant is given by

$$\lambda = \frac{\mu_0 \mu^2}{4\pi k_{\mathrm{B}} T d^3} = \frac{J}{2\varphi} \tag{5}$$

where μ_0 is the vacuum permeability, and $\varphi \sim (d/a)^3$ is the volume fraction of particles. For typical magnetic colloids, $\lambda \sim 1$ and $\varphi \sim 0.1$, so that in a random dispersion of particles, $J = 2\lambda\varphi \sim 0.2$. If the applied field strength is H, then the Langevin parameter is

$$\alpha = \frac{\mu_0 \mu H}{k_{\mathrm{B}} T}. \tag{6}$$

The initial susceptibility in the z direction is given by

$$\chi = \left(\frac{\partial M}{\partial H}\right)_{H=0} \tag{7}$$

where $M = m\mu/a^3$ is the real magnetization. In terms of the fractional magnetization m and the Langevin parameter α

$$\chi = \frac{\mu_0 \mu^2}{k_\mathrm{B} T a^3} \left(\frac{\partial m}{\partial \alpha} \right)_{\alpha=0}. \tag{8}$$

C. Yvon-Born-Green equation

The aim is to calculate the one-spin density $\rho(\boldsymbol{S})$, from which the magnetization curve and initial susceptibility can be obtained. The Yvon-Born-Green (YBG) equation linking the one-spin density to the pair distribution function $g(\boldsymbol{S}, \boldsymbol{S}', r)$ is [21]

$$\begin{aligned} \frac{\mathrm{d} \ln \rho(\boldsymbol{S})}{\mathrm{d}\boldsymbol{S}} &= -\frac{\mathrm{d}\beta\Phi(\boldsymbol{S})}{\mathrm{d}\boldsymbol{S}} \\ &- 2\sum_{r=1}^{R} \int \mathrm{d}\boldsymbol{S}' \frac{\mathrm{d}\beta U(\boldsymbol{S}, \boldsymbol{S}', r)}{\mathrm{d}\boldsymbol{S}} \rho(\boldsymbol{S}') g(\boldsymbol{S}, \boldsymbol{S}', r) \end{aligned} \tag{9}$$

where the factor of 2 in the second term on the right-hand side accounts for interactions between a spin and the R neighbors either side of it. The general approach is to use approximations for $\rho(\boldsymbol{S}')$ and $g(\boldsymbol{S}, \boldsymbol{S}', r)$, and to obtain simple, closed-form expressions for $\rho(\boldsymbol{S})$, m, and χ. Two different cases will be considered: zero anisotropy ($\sigma = 0$) meaning that the spins are free to rotate in all three directions; and infinite anisotropy ($\sigma = \infty$) meaning that the spins are constrained to lie parallel or antiparallel to the z axis.

D. Zero anisotropy

With $\sigma = 0$, the spins are free to point in any direction in space. Two theories will be summarized below: a modified mean-field theory based on non-interacting spins; and conventional Weiss mean-field theory [22].

1. *Modified mean-field theory based on non-interacting spins*

In what follows, the tilde ($\tilde{}$) denotes a reference system with known properties that are used to evaluate the right-hand side of the YBG equation. For non-interacting spins, the one-spin density is

$$\tilde{\rho}(\cos\theta) = \frac{\alpha \exp(\alpha \cos\theta)}{2 \sinh \alpha} \tag{10}$$

and the fractional magnetization is

$$\tilde{m} = \coth \alpha - \frac{1}{\alpha} \equiv L(\alpha) \tag{11}$$

which defines the Langevin function L. The initial susceptibility for non-interacting spins is

$$\chi_0 = \frac{\mu_0 \mu^2}{3 k_\mathrm{B} T a^3} \tag{12}$$

which is the equivalent of the Langevin susceptibility for magnetic colloids. There are no correlations between non-interacting spins, and hence the pair distribution function in this case is $\tilde{g}(\boldsymbol{S}, \boldsymbol{S}', r) = 1$. The YBG equation with $R = \infty$ is then

$$\begin{aligned} \frac{\mathrm{d} \ln \rho(\cos\theta)}{\mathrm{d} \cos\theta} &= \alpha + \sum_{r=1}^{\infty} \frac{2J}{r^3} \int_{-1}^{1} \cos\theta' \tilde{\rho}(\cos\theta') \mathrm{d}\cos\theta' \\ &= \alpha + 2J\zeta(3)\tilde{m} \end{aligned} \tag{13}$$

where $\zeta(3) = \sum_{r=1}^{\infty} 1/r^3 \simeq 1.20205$. Note that differentiating U with respect to $\cos\theta$ gives one term proportional to $\cos(\phi - \phi')$ that disappears on integration over ϕ', and another term proportional to $\cos\theta'$ that does not depend on ϕ' at all. Integrating the YBG equation gives the one-spin density

$$\rho(\cos\theta) = \frac{\alpha_\mathrm{eff} \exp(\alpha_\mathrm{eff} \cos\theta)}{2 \sinh \alpha_\mathrm{eff}} \tag{14}$$

and the magnetization curve

$$m = L(\alpha_\mathrm{eff}) \tag{15}$$

where

$$\alpha_\mathrm{eff} = \alpha + 2J\zeta(3)\tilde{m} \tag{16}$$

is the effective field felt by a single spin, containing the bare-field term α, and the interactions with all of the other spins. The susceptibility for interacting spins, compared to that for non-interacting spins, is given by

$$\frac{\chi}{\chi_0} = 3 \left(\frac{\partial m}{\partial \alpha} \right)_{\alpha=0} = 1 + \frac{2J\zeta(3)}{3}. \tag{17}$$

This theory is referred to as 'MMF(NI)', where 'NI' indicates that $\tilde{\rho}$ and $\tilde{g}$ are those of the non-interacting system.

2. *Mean-field theory*

Of course, the conventional Weiss mean-field theory [22] gives an effective field precisely of the form of Eq. (16), but with m determined self-consistently according to the relation

$$m = L(\alpha + 2J\zeta(3)m). \tag{18}$$

Linearizing this equation gives the result

$$\frac{\chi}{\chi_0} = \left[1 - \frac{2J\zeta(3)}{3} \right]^{-1} \tag{19}$$

which erroneously signals a transition to a ferromagnetic phase at $J_\mathrm{c} = 3/2\zeta(3) \simeq 1.24786$. Note that an expansion of this result with respect to J gives a linear term in agreement with Eq. (17). This theory is indicated with 'MF' for 'mean field'.

E. Infinite anisotropy

If a spin is strongly aligned with the z axis, then $S_{ix}^2 + S_{iy}^2 = \epsilon$ and $S_{iz} \approx \pm(1 - \frac{1}{2}\epsilon)$. It is necessary to keep $\boldsymbol{S}_i$ as a continuous variable in order to define and integrate the YBG equation. In the limit $\sigma \to \infty$, $\boldsymbol{S}_i = (0, 0, S_i)$ with $S_i = \pm 1$, and so the fractional magnetization is

$$m = \rho(+1) - \rho(-1) = 2\rho(+1) - 1 = 1 - 2\rho(-1) \quad (20)$$

and the one-spin density can be written

$$\tilde{\rho}(S) = \frac{1}{2}(1 + S\tilde{m})\left[\delta(S-1) + \delta(S+1)\right] \quad (21)$$

where S is constrained to ± 1 by the Dirac δ functions. The one-dimensional dipolar Ising model and extensions have been used to study inhomogeneous nanowires [23], structure in organic ferroelectrics [24], and the ordering of water in one-dimensional nanopores [25–27]. Three theories will be detailed below: two modified mean-field theories will be derived, based on non-interacting spins, and the nearest-neighbor Ising model; and the Weiss mean-field model.

1. *Modified mean-field theory based on non-interacting spins*

For non-interacting particles in the limit $\sigma \to \infty$, the one-spin density is

$$\tilde{\rho}(S) = \frac{\exp(\alpha S)\left[\delta(S-1) + \delta(S+1)\right]}{2\cosh\alpha} \quad (22)$$

the magnetization curve is

$$\tilde{m} = \tanh\alpha \quad (23)$$

and the pair distribution function is $\tilde{g}(S, S', r) = 1$. Hence, the YBG equation becomes

$$\begin{aligned} \frac{\mathrm{d}\ln\rho(S)}{\mathrm{d}S} &= \alpha + 2\sigma S + \sum_{r=1}^{\infty} \frac{2J}{r^3} \int_{-1}^{1} S'\tilde{\rho}(S')\mathrm{d}S' \\ &= \alpha + 2\sigma S + 2J\zeta(3)\tilde{m}. \end{aligned} \quad (24)$$

Integrating this equation gives

$$\ln\left[\frac{\rho(+1)}{\rho(-1)}\right] = 2\alpha + 4J\zeta(3)\tilde{m} \quad (25)$$

and hence

$$m = \frac{\frac{\rho(+1)}{\rho(-1)} - 1}{\frac{\rho(+1)}{\rho(-1)} + 1} = \tanh\alpha_{\mathrm{eff}} \quad (26)$$

where the effective field is

$$\alpha_{\mathrm{eff}} = \alpha + 2J\zeta(3)\tilde{m}. \quad (27)$$

The initial susceptibility is given by

$$\frac{\chi}{\chi_0} = \left(\frac{\partial m}{\partial\alpha}\right)_{\alpha=0} = 1 + 2J\zeta(3) \quad (28)$$

where for Ising-like spins

$$\chi_0 = \frac{\mu_0\mu^2}{k_{\mathrm{B}}Ta^3}. \quad (29)$$

This theory is referred to as 'MMF(NI)'.

2. *Modified mean-field theory based on interacting spins with $R = 1$*

Using a more accurate expression for the pair distribution function $\tilde{g}(S, S', r)$ should give improved results. To this end, $\tilde{\rho}(S')$ and $\tilde{g}(S, S', r)$ in the YBG equation can be approximated by the known functions for the nearest-neighbor Ising model [11], which corresponds to the current model with $R = 1$ and $\sigma = \infty$. The magnetization curve is given by

$$\tilde{m} = \frac{\sinh\alpha}{\sqrt{\exp(-4J) + \sinh^2\alpha}} \quad (30)$$

and the one-spin density is given by Eq. (21). As shown in the Appendix, the pair distribution function is given by

$$\tilde{g}(S, S', r) = \frac{1 + (S + S')\tilde{m} + SS'\tilde{C}_r}{(1 + S\tilde{m})(1 + S'\tilde{m})} \quad (31)$$

where $\tilde{C}_r$ is the spin-spin correlation function. $\tilde{C}_r$ is given by

$$\tilde{C}_r = \langle S_i S_{i+r}\rangle = \tilde{m}^2 + \left(\frac{\lambda_-}{\lambda_+}\right)^r \left(1 - \tilde{m}^2\right) \quad (32)$$

where

$$\lambda_\pm = e^J\cosh\alpha \pm \sqrt{e^{-2J} + e^{2J}\sinh^2\alpha}. \quad (33)$$

Now, these results are strictly for $S_i = \pm 1$, but to integrate the YBG equation, $\tilde{g}(S, S', r)$ should be a function of continuous variables. Therefore, the assumption is made that Eq. (31) applies for all values of $-1 \le S, S' \le 1$, and that the orientational correlations are independent of ϕ and ϕ'. With these assumptions, the YBG equation is

$$\begin{aligned} \frac{\mathrm{d}\ln\rho(S)}{\mathrm{d}S} &= \alpha + 2\sigma S + \sum_{r=1}^{\infty} \frac{2J}{r^3} \int_{-1}^{1} S'\tilde{\rho}(S')\tilde{g}(S, S', r)\mathrm{d}S' \\ &= \alpha + 2\sigma S + \sum_{r=1}^{\infty} \frac{2J}{r^3} \left(\frac{\tilde{m} + S\tilde{C}_r}{1 + S\tilde{m}}\right). \end{aligned} \quad (34)$$

Integrating this expression and using Eq. (26) gives a magnetization curve with an effective field

$$\alpha_{\text{eff}} = \alpha + \sum_{r=1}^{\infty} \frac{J}{r^3} \left[\left(1 - \frac{\tilde{C}_r}{\tilde{m}^2}\right) \ln\left(\frac{1+\tilde{m}}{1-\tilde{m}}\right) + \frac{2\tilde{C}_r}{\tilde{m}} \right]. \tag{35}$$

In a strong field and/or at large distances, $\tilde{C}_r \approx \tilde{m}^2$, and hence $\alpha_{\text{eff}} \approx \alpha + 2J\zeta(3)\tilde{m}$, which agrees with the MMF theory based on non-interacting spins [Eq. (27)]. The initial susceptibility is given by

$$\frac{\chi}{\chi_0} = 1 + 2J\zeta(3)\left(\frac{1+\tanh J}{1-\tanh J}\right) \tag{36}$$

where $\chi_0(1+\tanh J)/(1-\tanh J)$ is the initial susceptibility of the Ising model with $R = 1$. This theory is referred to as 'MMF($R = 1$)', which indicates that $\tilde{\rho}$ and $\tilde{g}$ are those of the system with $R = 1$.

3. *Mean-field theory*

Solving the linearized version of the self-consistent equation

$$m = \tanh\left(\alpha + 2J\zeta(3)m\right) \tag{37}$$

gives for the initial susceptibility

$$\frac{\chi}{\chi_0} = \frac{1}{1 - 2J\zeta(3)} \tag{38}$$

which predicts a critical coupling constant $J_c = 1/2\zeta(3) \simeq 0.415954$. It is known that there is no phase transition for the one-dimensional dipolar Ising model [15–19]. The linearized version of this formula agrees with the MMF result in Eq. (28). This theory is referred to as 'MF'.

III. MONTE CARLO SIMULATIONS

To test the accuracy of the theories, MC simulations were carried out on chains of $N = 1000$ spins, with periodic boundary conditions applied [28]. One MC sweep consisted of N attempted rotations of randomly selected spins. With $\sigma = 0$, a spin was rotated about a randomly generated axis by a randomly chosen angle in the range $[-\pi, \pi]$. With $\sigma = \infty$, a spin was flipped from S to $-S$. Each simulation consisted of between 1×10^5 and 1×10^6 MC sweeps, depending on the parameters R, J, and α. The initial susceptibility was calculated using the standard fluctuation formula

$$\frac{\chi}{\chi_0} = \frac{n\left\langle M^2\right\rangle}{N} \tag{39}$$

where $M = \sum_{i=1}^{N} S_{iz}$, $n = 3$ for $\sigma = 0$, and $n = 1$ for $\sigma = \infty$.

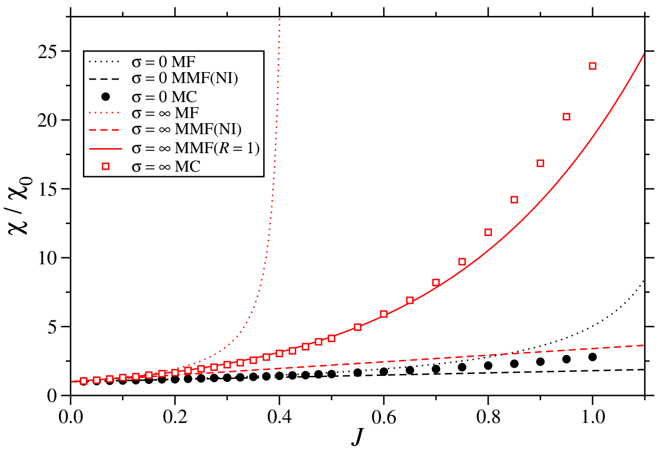

FIG. 1. The ratio χ/χ_0 as a function of J for systems with $\sigma = 0$ and $\sigma = \infty$. The points are from MC simulations, and the lines are from theory: MF theory with $\sigma = 0$ (black dotted line); MMF(NI) theory based on non-interacting spins with $\sigma = 0$ (black dashed line); MC simulations with $\sigma = 0$ (black filled circles); MF theory with $\sigma = \infty$ (red dotted line); MMF(NI) theory based on non-interacting spins with $\sigma = \infty$ (red dashed line); MMF($R = 1$) theory based on interacting spins with $R = 1$ and $\sigma = \infty$ (red solid line); MC simulations with $\sigma = \infty$ (red unfilled squares).

IV. RESULTS

Fig. 1 shows the ratio χ/χ_0 as a function of J for models with $\sigma = 0$ and $\sigma = \infty$. The initial susceptibility with $\sigma = \infty$ increases much more rapidly than that with $\sigma = 0$, because the spins are constrained to lie parallel or antiparallel to the z axis. With $\sigma = 0$, both the MF theory and the MMF(NI) theory are in reasonable agreement with the MC simulation results. The MF theory predicts a divergence in χ at $J_c \simeq 1.24786$, which is an artifact. With $\sigma = \infty$, the MF theory predicts a divergence at $J_c \simeq 0.415954$, which renders it highly inaccurate except at very low values of J. The two MMF theories perform very differently. The MMF(NI) theory is only accurate at low values of J, while the MMF($R = 1$) theory is accurate up to $J \simeq 0.7$. This shows that including correlations has a huge effect on the results for systems with strong anisotropy.

Near the critical temperature T_c, the initial susceptibility follows the scaling law $\chi \sim (T - T_c)^{-\gamma}$, where γ is a critical exponent that depends on the universality class of the Hamiltonian [29]. The classical Curie-Weiss law of (anti)ferromagnetism states that $1/\chi \propto (T - T_c)$. In the present case, $T_c = 0$ because there is no long-range order at finite temperature. Since $\chi_0 \propto J$ [Eqs. (12) and (29)], it is clear that $1/\chi \propto \chi_0/J\chi$. Fig. 2 shows a plot of $\chi_0/J\chi$ as a function of the dimensionless temperature $1/J$. These plots show that, at high temperature, the initial susceptibility follows the Curie-Weiss law. MC simulations show that, at low temperature, the susceptibility does not diverge according to any scaling law, since

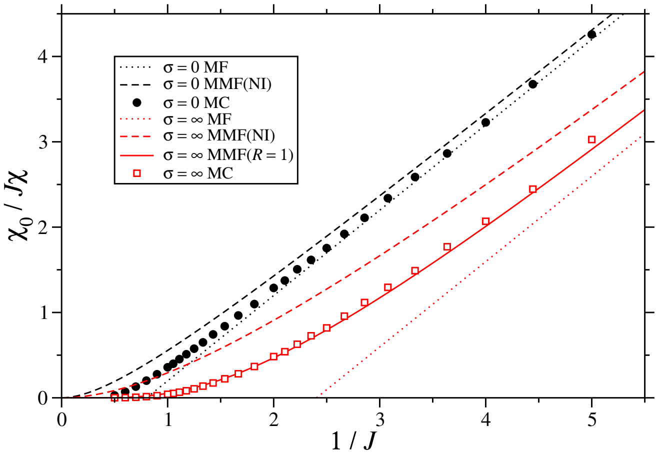

FIG. 2. The ratio $\chi_0/J\chi$ as a function of $1/J$ for systems with $\sigma = 0$ and $\sigma = \infty$. The points are from MC simulations, and the lines are from theory: MF theory with $\sigma = 0$ (black dotted line); MMF(NI) theory based on non-interacting spins with $\sigma = 0$ (black dashed line); MC simulations with $\sigma = 0$ (black filled circles); MF theory with $\sigma = \infty$ (red dotted line); MMF(NI) theory based on non-interacting spins with $\sigma = \infty$ (red dashed line); MMF($R = 1$) theory based on interacting spins with $R = 1$ and $\sigma = \infty$ (red solid line); MC simulations with $\sigma = \infty$ (red unfilled squares).

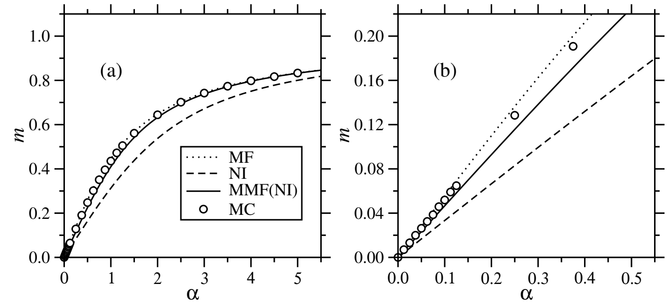

FIG. 3. The magnetization curve with $\sigma = 0$ and $J = 0.5$: (a) expanded scale; (b) linear-response regime. The points are from MC simulations, and the lines are from theory: MF theory (dotted line); non-interacting (NI) spins (dashed line); MMF(NI) theory based on non-interacting spins (solid line).

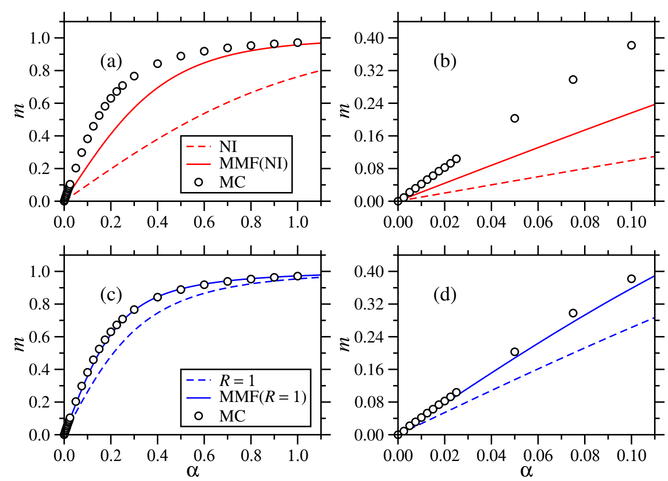

FIG. 4. The magnetization curve with $\sigma = \infty$ and $J = 0.5$: (a) and (c) expanded scale; (b) and (d) linear-response regime. The points are from MC simulations, and the lines are from theory: (a) and (b) non-interacting (NI) spins (red dashed line); (a) and (b) MMF(NI) theory based on non-interacting spins (red solid line); (c) and (d) interacting spins with $R = 1$ (blue dashed lines); (c) and (d) MMF($R = 1$) theory based on interacting spins with $R = 1$ (blue solid line).

there is no phase transition in these models. The MF theories for both $\sigma = 0$ and $\sigma = \infty$ erroneously signal phase transitions. With $\sigma = 0$, both the MF theory and the MMF(NI) theory are in good agreement with the simulation results at high temperature. With $\sigma = \infty$, the superiority of the MMF($R = 1$) theory over the MF and MMF(NI) theories is clear. All of the MMF theories are qualitatively correct in that they do not predict a phase transition at finite temperature.

Figs. 1 and 2 show that with a moderate value of $J = 0.5$, the $\sigma = 0$ case is well described by both the MF and MMF(NI) theories. Fig. 3 shows the magnetization curve for this case, on both an expanded scale ($\alpha \leq 5$) and in the linear-response regime ($\alpha \leq 0.5$). The magnetization curve for the non-interacting system [Eq. (11)] is clearly inadequate. Both the MMF(NI) theory [Eq. (15)] and the the MF theory [Eq. (18)] are in good agreement with the MC simulations, and there is not much to choose between them. The MF theory slightly overestimates the initial susceptibility, while the MMF(NI) slightly underestimates it.

Figs. 1 and 2 show that the $\sigma = \infty$ case demands a more sophisticated theory. The magnetization curve with $J = 0.5$ is shown in Fig. 4. For clarity, Fig. 4(a) and (b) show the results for non-interacting spins and from MMF(NI) theory, and Fig. 4(c) and (d) show the results for interacting spins with $R = 1$ and from MMF($R = 1$) theory. The comparisons with MC simulation results are made on both expanded scales [(a) and (c)] and in the linear-response regime [(b) and (d)]. The MF theory is not shown because $J = 0.5$ is above the apparent value of J_c. The results for non-interacting spins and from MMF(NI) are not in good agreement with the MC simulation data. The MMF($R = 1$) theory, however, shows excellent agreement with the MC simulations.

Fig. 5 shows a direct comparison of the MMF(NI) and MMF($R = 1$) theories for systems with $\sigma = \infty$ and $J = 0.25$, 0.50, and 1.00. The results show that the deviation between the two theories grows rapidly with increasing J. With $J = 0.25$ and 0.50, the MMF($R = 1$) theory is essentially perfect. Even with $J = 1.00$, where the initial susceptibility is not very accurate, the MMF($R = 1$) theory is in moderate agreement with the MC simulation results.

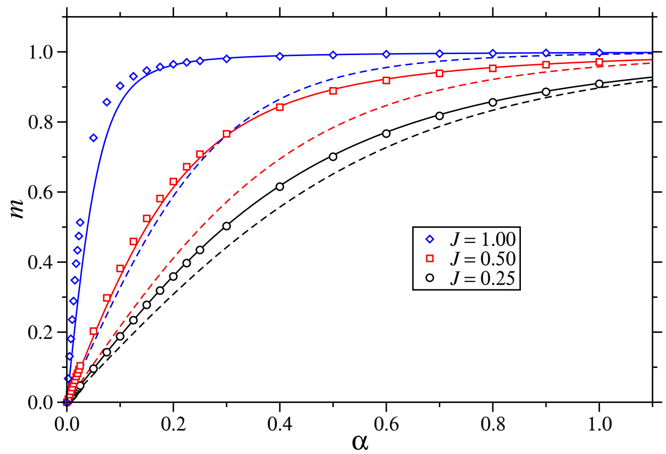

FIG. 5. The magnetization curves with $\sigma = \infty$ and $J = 0.25$, 0.50, and 1.00. The points are from MC simulations: $J = 0.25$ (black circles); $J = 0.50$ (red squares); $J = 1.00$ (blue diamonds). The lines are from theory: MMF(NI) theory based on non-interacting spins (dashed lines); MMF($R = 1$) theory based on interacting spins with $R = 1$ (solid lines).

V. CONCLUSIONS

Motivated by a recent study of the magnetic properties of immobilized superparamagnetic particles [4], this work was devoted to the influence of the anisotropy in one-dimensional spin models with long-range dipolar interactions. Various theories were tested against computer-simulation results for the initial susceptibility and the magnetization curve. It was shown that increasing the anisotropy (and changing from Heisenberg-like to Ising-like spins) increases the initial susceptibility, in line with earlier work. Self-consistent mean-field theory and a modified mean-field theory based on non-interacting spins (no correlations) work quite well in the case of zero anisotropy. Physically, this is due to the unhindered rotation of the spins, and the fact that the effective dipolar interactions become short-ranged. In the limit of infinite anisotropy, both of these theories fail badly with strong interactions between the spins. A modified mean-field theory based on spins with nearest-neighbor interactions was shown to work extremely well. The inclusion of strong ferromagnetic correlations, albeit approximately, gives a much more accurate estimation of the effective field felt by an individual spin, modified by long-range interactions with the other spins. The resulting formulas for the magnetization curve and initial susceptibility are simple and in closed form. It is hoped that a similar approach can be found to treat spatially disordered systems such as strongly interacting ferrofluids, ferrogels, and composites with immobilized superparamagnetic particles.

ACKNOWLEDGMENTS

The authors are honored to contribute to this special issue celebrating Professor Leonid Bulavin's 75$^{\text{th}}$ birthday. The authors' collaboration began after they met at the 2005 *Physics of Liquid Matter: Modern Problems* conference in Kyiv, organized by Professor Bulavin. P.J.C. thanks the Ural Federal University for supporting collaborative visits between Edinburgh and Ekaterinburg. The research was carried out within the state assignment of the Ministry of Science and Higher Education of the Russian Federation (theme "Magnet" and Contract No. 02.A03.21.006).

Appendix: Pair distribution function of the nearest-neighbor Ising model

The pair distribution function is defined as [21]

$$\tilde{g}(S,S',r) = \frac{\tilde{\rho}(S,S',r)}{\tilde{\rho}(S)\tilde{\rho}(S')} \tag{A.1}$$

where $\tilde{\rho}(S)$ and $\tilde{\rho}(S,S',r)$ are, respectively, the one-spin and two-spin densities. The two-spin density must fulfill the following four conditions.

$$\sum_S \sum_{S'} \tilde{\rho}(S,S',r) = 1 \tag{A.2a}$$

$$\sum_S \sum_{S'} (S+S')\tilde{\rho}(S,S',r) = 2\tilde{m} \tag{A.2b}$$

$$\sum_S \sum_{S'} SS'\tilde{\rho}(S,S',r) = \tilde{C}_r \tag{A.2c}$$

$$\tilde{\rho}(+1,-1,r) = \tilde{\rho}(-1,+1,r) \tag{A.2d}$$

These conditions allow the computation of the four values of $\tilde{\rho}(S,S',r)$ from the known functions $\tilde{m}$ [Eq. (30)] and $\tilde{C}_r$ [Eq. (32)].

$$\tilde{\rho}(+1,+1,r) = \frac{1}{4}\left(1 + 2\tilde{m} + \tilde{C}_r\right) \tag{A.3a}$$

$$\tilde{\rho}(+1,-1,r) = \tilde{\rho}(-1,+1,r) = \frac{1}{4}\left(1 - \tilde{C}_r\right) \tag{A.3b}$$

$$\tilde{\rho}(-1,-1,r) = \frac{1}{4}\left(1 - 2\tilde{m} + \tilde{C}_r\right) \tag{A.3c}$$

Combining these relations with $\tilde{\rho}(S) = \frac{1}{2}(1 + S\tilde{m})$ gives Eq. (31).

Fig. 6 shows examples of $\tilde{g}(S,S',r)$ for systems with $R = 1$, $J = 0.5$, and $\alpha = 0.0$ and 0.2, from MC simulations and Eq. (31). The agreement between theory and simulation is perfect. In zero field ($\alpha = 0$), $g(1,1,r) = g(-1,-1,r)$, and these ferromagnetic correlations are stronger than the antiferromagnetic ones [$g(1,-1,r) = g(-1,1,r)$]. In an applied field ($\alpha > 0$), most spins are parallel to the field and hence $g(1,1,r) \simeq 1$, while pairs of spins antiparallel to the field are attracted to one another [$g(-1,-1,r)$], and spins opposite to one another are repelled [$g(1,-1,r) = g(-1,1,r)$].

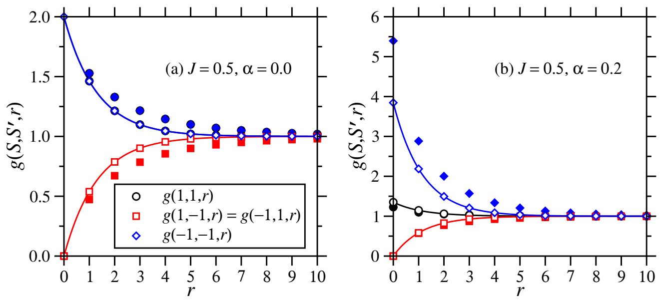

FIG. 6. Pair distribution functions with $\sigma = \infty$: (a) $J = 0.5$ and $\alpha = 0.0$; (b) $J = 0.5$ and $\alpha = 0.2$. The unfilled symbols are for the nearest-neighbor Ising model ($R = 1$), and the filled symbols are for the long-range dipolar model ($R = \infty$). The lines are for the system with $R = 1$, from Eq. (31).

Fig. 6 also shows the pair distribution functions for systems with long-range dipolar interactions ($R = \infty$), calculated in MC simulations. The results show that the correlations are qualitatively similar, but longer ranged, as expected.

[1] R. E. Rosensweig, *Ferrohydrodynamics* (Dover Publications, Inc., New York, 1998).

[2] J. Carrey, B. Mehdaoui, and M. Respaud, "Simple models for dynamic hysteresis loop calculations of magnetic single-domain nanoparticles: Application to magnetic hyperthermia optimization," J. Appl. Phys. **109**, 083921 (2011).

[3] A. L. Elrefai, T. Sasayama, T. Yoshida, and K. Enpuku, "Empirical expression for DC magnetization curve of immobilized magnetic nanoparticles for use in biomedical applications," AIP Advances **8**, 056803 (2018).

[4] E. A. Elfimova, A. O. Ivanov, and P. J. Camp, "Static magnetization of immobilized, weakly interacting, superparamagnetic nanoparticles," Nanoscale **11**, 21834–21846 (2019).

[5] A. O. Ivanov and O. B. Kuznetsova, "Magnetic properties of dense ferrofluids: An influence of interparticle correlations," Phys. Rev. E **64**, 041405 (2001).

[6] A. O. Ivanov and O. B. Kuznetsova, "Magnetogranulometric analysis of ferrocolloids: Second-order modified mean field theory," Colloid J. **68**, 430–440 (2006).

[7] W. H. Keesom, "On the deduction from Boltzmann's entropy principle of the second virial-coefficient for material particles (in the limit rigid spheres of central symmetry) which exert central forces upon each other and for rigid spheres of central symmetry containing an electric doublet at their centers," Comm. Phys. Lab. Leiden, Suppl. **24b**, 23–41 (1912).

[8] H. E. Stanley, "Dependence of critical properties on dimensionality of spins," Phys. Rev. Lett. **20**, 589–592 (1968).

[9] M. E. Fisher, "Magnetism in one-dimensional systems–the Heisenberg model for infinite spin," Am. J. Phys. **32**, 343–346 (1964).

[10] G. S. Joyce, "Classical Heisenberg model," Phys. Rev. **155**, 478–491 (1967).

[11] R. J. Baxter, *Exactly Solved Models in Statistical Mechanics* (Academic Press Limited, London, 1982).

[12] N. D. Mermin and H. Wagner, "Absence of ferromagnetism or antiferromagnetism in one- or two-dimensional isotropic Heisenberg models," Phys. Rev. Lett. **17**, 1133–1136 (1966).

[13] J. Frölich, R. Israel, E. H. Lieb, and B. Simon, "Phase transitions and reflection positivity. I. General theory and long range lattice models," Commun. Math. Phys. **62**, 1–34 (1978).

[14] P. Bruno, "Absence of spontaneous magnetic order at nonzero temperature in one- and two-dimensional Heisenberg and XY systems with long-range interactions," Phys. Rev. Lett. **87**, 137203 (2001).

[15] D. Ruelle, "Statistical mechanics of a one-dimensional lattice gas," Commun. Math. Phys. **9**, 267–278 (1968).

[16] F. J. Dyson, "Existence of a phase-transition in a one-dimensional Ising ferromagnet," Commun. Math. Phys. **12**, 91–107 (1969).

[17] F. J. Dyson, "Non-existence of spontaneous magnetization in a one-dimensional Ising ferromagnet," Commun. Math. Phys. **12**, 212–215 (1969).

[18] F. J. Dyson, "An Ising ferromagnet with discontinuous long-range order," Commun. Math. Phys. **21**, 269–283 (1971).

[19] J. Frölich and T. Spencer, "The phase transition in the one-dimensional Ising model with $1/r^2$ interaction energy," Commun. Math. Phys. **84**, 87–101 (1982).

[20] T. Morita and T. Horiguchi, "Classical one-dimensional Heisenberg model with an interaction of finite range," Physica A **83**, 519–532 (1976).

[21] J.-P. Hansen and I. R. McDonald, *Theory of Simple Liquids*, 3rd ed. (Academic Press, London, 2006).

[22] P. Weiss, "L'hypothese du champ moleculaire et la propriete ferromagnetique," J. Phys. Theor. Appl. **6**, 661–690 (1907).

[23] M. Eisenbach, M. Dijkstra, and B. L. Györffy, "On the states of orientations along a magnetically inhomogeneous nanowire," J. Mag. Magn. Mater. **208**, 137–143 (2000).

[24] Y. Yamamura, H. Saitoh, M. Sumita, and K. Saito, "One-dimensional correlation in the dipolar Ising crystal tricyclohexylmethanol: crystal structure revisited and heat capacity," J. Phys.: Condens. Matter **19**, 176219 (2007).

[25] J. Köfinger, G. Hummer, and C. Dellago, "Macroscopically ordered water in nanopores," Proc. Natl. Acad. Sci. U.S.A. **105**, 13218–13222 (2008).

[26] J. Köfinger, G. Hummer, and C. Dellago, "A one-dimensional dipole lattice model for water in narrow

nanopores," J. Chem. Phys. **130**, 154110 (2009).

[27] J. Köfinger and C. Dellago, "Single-file water as a one-dimensional Ising model," New J. Phys. **12**, 093044 (2010).

[28] K. Binder and D. P. Landau, *A Guide to Monte Carlo Simulations in Statistical Physics*, 2nd ed. (Cambridge University Press, Cambridge, 2005).

[29] H. E. Stanley, *Introduction to Phase Transitions and Critical Phenomena*, International Series of Monographs on Physics (Oxford University Press, New York, 1971).